Three-dimensional FE/NCV Simulation of Pultrusion Process with Temperature-dependent Material Properties including Resin Shrinkage

Joshi, Sunil Chandrakant; Lam, Yee Cheong

2001

Joshi, S. C., & Lam, Y. C. (2015). Three-dimensional FE/NCV Simulation of Pultrusion Process with Temperature-dependent Material Properties including Resin Shrinkage. Composites Science and Technology, 61(11), 1536-1547.

https://hdl.handle.net/10356/80822

https://doi.org/10.1016/S0266-3538(01)00056-2

Three-dimensional FE/NCV simulation of pultrusion process with temperature-dependent material properties including resin shrinkage

Sunil C. Joshi* **and Y.C. Lam**

School of Mechanical & Production Engineering,
Nanyang Technological University, Singapore 639 798.

ABSTRACT: *This paper discusses the development and application of the finite element/ nodal control volume (FE/NCV) approach for three-dimensional pultrusion analysis. A numerical procedure is designed using a combination of the field analysis module of a general-purpose finite element package and a few user-written computer codes. Numerical schemes employed for calculating the convective heat transfer effects on temperature and degree of cure, for modelling resin cure kinetics and the effects of temperature-dependent material properties, and for determining the dimensional changes due to chemical shrinkage and thermal expansion of resin are discussed in detail. Case studies are presented demonstrating the simulation of pultrusion process for different components including irregular and hollow sections.*

KEY WORDS: A: Polymer-matrix composites; C: Computational simulation; C: Finite element analysis; E: Pultrusion; Nodal control volumes.

* Author for correspondence: mscjoshi@ntu.edu.sg; Phone: (65) 790 5954; Fax: (65) 791 1859.

1. INTRODUCTION

Pultrusion is one of the manufacturing processes used for continuous fabrication of fibre-reinforced polymer composites of constant cross-section. In this process, dry fibreous reinforcement is pulled through a resin bath for resin impregnation. Upon wetting the reinforcement is allowed to enter a heated die where it acquires the shape of the die cavity and cures sufficiently before it is cut into the required lengths. As mechanical performance of a pultruded part depends upon the quality of its cure, understanding heat and mass transfer and curing of the composites in a pultrusion die is extremely important. In the past, many researchers [1-5] have used computer simulation to study these phenomena in pultrusion.

While modelling the pultrusion process, unlike other researchers, Suratno et al. [1] and Liu et al. [2] employed a general-purpose finite element (FE) package to perform heat transfer analysis and developed either user-routines or computer-codes using various numerical schemes to solve the cure kinetics and the species equation. Similar approach was also used in the past for the simulation of prepreg moulding [6], resin transfer moulding [7,8] and resin-film infusion [9] processes. The obvious advantage of this approach is that no special FE code, which constitutes a major part of the simulation procedure, needs to be developed for conducting heat transfer analysis. In addition, user-friendly pre- and post-processors and available element libraries of commercial FE packages increase the convenience of modelling irregular shapes and hollow sections in three-dimensions. Also, a variety of boundary conditions and material properties can be defined easily.

Suratno et al. [1] used an approximate numerical scheme to model resin cure kinetics. The results of their studies were found to be sensitive to Peclet number (P_e), which depends on the length of the finite element along the pull direction (L), the pull speed (w), the thermal mass ($\rho_c C_{pc}$) and the conductivity (k_c) of the composites. Liu et al. [2] used the

concept of nodal control volume (NCV) to simulate resin cure reaction and the convective effects on temperature and cure. This FE/NCV approach was found to be more robust, numerically stable, and was not sensitive to the element size.

However, the effects of temperature-dependent material properties and shrinkage of the composites part were not considered by these researchers. The modelling of hollow, irregular shaped components with an internal die was also not attempted.

Thermal properties λ and C_p of a thermosetting resin change with temperature and state of cure, and the properties in a fully cured state could be *30-40*% higher than that in an uncured state [10,11]. If overlooked, such a high variation in resin properties may lead to erroneous results during process simulation. In pultrusion, as the resin cures, composites part separates from die wall due to resin shrinkage [11] and the rate of heat transfer between a die and a component, the uniformity of resin cure and the dimensions of a pultruded part are significantly affected. Therefore, in order to make precise predictions about the quality and the final dimensions of a pultrudate, the effects of thermal expansion and shrinkage of resin should not be ignored during simulation. However, a more comprehensive simulation procedure is required to account for these effects. Although the pultrusion process is commonly used for fabricating hollow and irregular composite sections with internal dies, the process simulation is difficult because of the multiple surfaces available for heat transfer. The difficulties are expected to increase further when the changes in the dimensions of a hollow pultrudate are to be determined while curing is still in progress.

In the present investigation, a FE/NCV numerical procedure for three-dimensional simulation of the pultrusion process was developed. The field analysis module of a FE package, (LUSAS, v13.0), was employed to perform conductive heat transfer analysis. The heat transfer between an immovable die and a continuously moving composites part through the die cavity was modelled using thermal surfaces. A few numerical schemes were developed

to cater for the changes in material properties and their effects as a function of temperature. Based on the concept of NCV, a semi-numerical scheme was contrived for predicting dimensional changes in the composites part during the analysis. A number of FORTRAN codes were written based on these numerical schemes. Capabilities to use hexahedron and pentahedron finite elements were included so that complex shapes can be modelled easily. These computer programs were employed in combination with LUSAS to perform iterative analysis in a batch mode.

A few case studies were carried out to validate the developed procedure. The example on a bridge deck section with internal die was included to demonstrate the usefulness and the capability of the developed numerical procedure in modelling pultrusion of irregular and hollow sections.

2. THEORITICAL BACKGROUND

2.1 Governing Equations

With the assumption that a fibrous medium impregnated with incompressible resin forms a macroscopically homogeneous material system for heat transfer analysis, the three-dimensional energy equation for a moving composites lay-up in a pultrusion die may be written as:

$$\rho_c C_{pc}\left(\frac{\partial T}{\partial t} + w\frac{\partial T}{\partial z}\right) = \nabla(\bar{k}_c \nabla T) + \frac{\partial H}{\partial t} \qquad (1)$$

where T is the temperature, H the heat energy and t the time. The ∇ denotes differential operator and Z the pull direction. The term $\frac{\partial H}{\partial t}$ defines the rate of internal heat generation in the composites, which for the case of thermosetting resin represents the heat of exothermic cure reaction. By substituting $w = 0$, Equation (1) can be used to express heat transfer in a

non-moving die section, where $\frac{\partial H}{\partial t}$ would represent the rate at which heating power is supplied to or lost from the die.

When a composites mass containing reactive resin moves through a die, the conservation of chemical species can be expressed as [7]:

$$\frac{\partial \alpha}{\partial t} + w\frac{\partial \alpha}{\partial z} = \dot{R}_\alpha \tag{2}$$

where α, the degree of cure (DOC), is defined as the ratio of the heat released to the total heat of cure reaction. $\dot{R}_\alpha$ is the rate of cure reaction. The relationship between $\frac{d\alpha}{dt}$, T and α can be approximated using an Arrehenius equation as [6]:

$$\frac{d\alpha}{dt} = B_0 \exp\left(\frac{-\Delta E}{RT}\right)(1-\alpha)^n \tag{3}$$

where B_0 is the pre-exponential constant, ΔE the activation energy, R the universal gas constant, and n the order of reaction. The $\frac{dH}{dt}$ for a resin saturated preform is directly proportional to $\dot{R}_\alpha$, and these two terms can be related by an equation as [6]:

$$\frac{dH}{dt} = \rho_r v_r H_t \dot{R}_\alpha \tag{4}^{\oplus}$$

where H_t is the total heat of reaction per unit mass of resin, v the volume fraction, and the subscript r denotes the matrix (resin).

2.2 Field analysis

Field theory is a unified theory that deals with a number of different physical situations characterized by Laplace's equation ($\nabla^2\phi = 0$) or its variants. It can describe not only the

$^{\oplus}$ In [6], variable ρ_c appeared in Equation (2) inadvertently due to a typographical error. In the same reference, for numerical implementation of Equation (2), Equation (11) is correct without ρ_c.

inverse square law of force (gravitational, magnetic or electric), but also conductive heat transfer, electric current flow, fluid flow, seepage or flow through permeable media [12]. Many commercial FE packages contain a field analysis module because of its wide application. For example, the following equation is solved for transient field analysis in LUSAS [13]:

$$\nabla\left[S_i(\phi)\nabla\phi\right] + H(\phi) = \rho\, C_p(\phi)\frac{\partial\phi}{\partial t} \tag{5}$$

where, typically for thermal conduction, ϕ, $S_i(\phi)$ and $H(\phi)$ represent T, $\bar{k}$ and $\frac{\partial H}{\partial t}$ respectively.

3. FE/ NCV MODELLING

The FE/NCV discretization of a pultrusion die and a component is shown in Figure 1. In FE analysis, a domain of interest is divided into a number of finite elements, each of them is defined with a set of nodal points. Within each finite element, the distribution of a field variable (e.g. temperature) is approximated using locally defined polynomials. Depending on the number of nodes, a set of equations is built and then solved to get the distribution of a field variable within the whole domain. A number of sub-control volumes are created within a zone defining polymer composites by connecting the centroid of a finite element to the centre points of its surfaces. The boundary of each sub-control volume contains only one FE node and all the sub-control volumes surrounding the node form a nodal control volume, which is represented by that particular node. In a control volume the distribution of a field variable is assumed constant and its value is defined by the field variable calculated at the representative FE node.

In pultrusion modelling, movement of resin-saturated composites preform is simulated as a semi-steady process. For a control volume, T, $\frac{d\alpha}{dt}$ and α are assumed constant over a small time-increment Δt. The exothermic effects of cure reaction, evaluated as $\frac{\partial H}{\partial t}$ using Equation (4), are added to Equation (5) as a source term. For each control volume the convective effects on temperature and DOC resulting from the movement of a composites lay-up in a hot die are included by calculating the terms $w\frac{\partial T}{\partial z}$ of Equation (1) and $w\frac{\partial \alpha}{\partial z}$ of Equation (2) respectively, and then superimposing them onto the results for the previous time step. The numerical schemes used to account for these effects are discussed below.

3.1 Heat of exothermic resin cure reaction

The following two integration schemes are commonly used to calculate DOC for a control volume [6].

In the forward integration scheme, the integral of Equation (3) can be evaluated approximately from α^j, the DOC of control volume j at the previous time-step i, as:

$$\alpha_{i+1}^j = \alpha_i^j + (t_{i+1} - t_i)\frac{\partial \alpha_{i,i+1}^j}{\partial t} \tag{6}$$

This scheme is easy to use and independent of the form of the cure kinetics equation. However, success of this scheme depends upon the maximum number of iterations allowed and the length of the time step employed for analysis.

Equation (3) can be also mathematically integrated using Vergnaud's integration scheme, by which we get:

$$\alpha_{i+1}^j = 1 - [1 + (n-1)S_{i+1}^j]^{\frac{1}{1-n}} \quad (n \neq 1) \tag{7}$$

where *S* is the integral and can be evaluated approximately as:

$$S_{i+1}^{j} = S_{i}^{j} + B_0 e^{(\frac{-\Delta E}{RT_i^j})}(t_{i+1} - t_i) \tag{8}$$

Although this scheme gives a better approximation, it cannot be used when the cure kinetics model is too complex to integrate mathematically.

Thus, once $\frac{d\alpha}{dt}$ and α for control volume j are known, $\frac{dH}{dt}$ can be calculated using Equation (4) and applied as a source term at node j.

3.2 Convective effects on temperature

According to the principle of energy conservation, every control volume should satisfy energy equilibrium at all time. The energy balance for a control volume depends upon its original temperature and the thermal energy flowing in or out of it. Thus, when over a small time increment Δt, a volume of composites ΔV^j, moves from control volume $j-1$ to control volume j (Figure 1), and the same amount of composites leaves j, the energy balance may be written as:

$$\rho_c^j C_{pc}^j V^j T^j + \Delta V^j \left[(\rho_c^{j-1} C_{pc}^{j-1} T^{j-1}) - (\rho_c^j C_{pc}^j T^j)\right] = \rho_c^j C_{pc}^j V^j (T^j + \Delta T^j) \tag{9}$$

where, $\Delta V^j = wA^j \Delta t$, $V^j = L^j A^j$, and A^j represents the cross-sectional area of control volume j. For the case of hexahedron control volumes, as shown in Figure 1, $A^j = W^j D^j$. With these conventions, Equation (9) can be further simplified to obtain ΔT^j as:

$$\Delta T^j = \lambda^j (\psi^j T^{j-1} - T^j) \tag{10}$$

where, $\lambda^j = \frac{\Delta V^j}{V^j} = \frac{w\Delta t}{L^j}$ and $\psi^j = \frac{\rho_c^{j-1} C_{pc}^{j-1}}{\rho_c^j C_{pc}^j}$. The value of λ^j indicates whether the control volume has moved by a distance equal to its full length over Δt or not. ψ^j represents the ratio of thermal mass of control volumes $j-1$ and j. Finally, the calculated ΔT^j is added to T^j to obtain the current temperature of control volume j, T_T^j.

3.3 Convective effects on Resin Cure

When a mass of composites moves to or from a control volume, state of cure of the control volume changes in the same proportion as that of the mass. Therefore, the concept of volume averaging can be used to calculate such a change in α for control volume j, $\Delta\alpha^j$, as:

$$\Delta\alpha^j = \frac{\Delta V^j}{V^j}(\alpha^{j-1} - \alpha^j) = \lambda^j(\alpha^{j-1} - \alpha^j) \tag{11}$$

The sum of $\Delta\alpha^j$ and α^j gives the final DOC of control volume j, α_T^j.

3.4 Dimensional changes

Thermal expansion of resin depends on its temperature and volumetric shrinkage of resin is a function of DOC [5,11]. If control volume j is fully filled with resin, the change in a unit dimension of the control volume due to these effects, δ_r^j, may be calculated as:

$$\delta_r^j = \left[1 + \varepsilon_r(T_T^j - T_0^j)\right] \times \left(1 - \frac{\gamma_r \alpha_T^j}{100}\right)^{\frac{1}{3}} \tag{12}$$

where, ε_r is the coefficient of thermal expansion, and γ_r is the percentage volumetric shrinkage of resin.

It may be observed from Equation (12) that when a composites part is being cured in a die, its dimensions change continuously. In the present approach, it is assumed that during pultrusion only the cross-sectional (i.e. X and Y) dimensions of a pultrudate change and the axis of gravity of the component (i.e. the Z-axis along which the pultrudate is moving) acts as a zero-shrinkage axis about which these changes take place. This assumption is valid because the continuous lengths of fibre reinforcement and the applied pulling force allow very little dimensional changes due to thermal expansion and shrinkage of resin in the longitudinal direction.

Before the analysis starts, the coordinates of the zero-shrinkage axis (i.e. X and Y coordinates of the Z-axis) are supplied as input data. During analysis, after each time step, the new dimensions of control volume j are calculated by multiplying its original dimensions by factor δ_c^j, calculated from δ_r^j, assuming that the fibres contribute little to the dimensional changes, as:

$$\delta_c^j = v_r \delta_r^j + v_f = 1 - v_r (1 - \delta_r^j) \tag{13}$$

The new X and Y coordinates of a FE node are then calculated by summing the corresponding new dimensions of all the control volumes that lie on the line joining the gravity axis and that particular FE node. Thus, at the end of each time step the changes in the shape and size of the component at all the cross-sections that lie within the forming die are calculated. The updated nodal coordinates are then used to drive the subsequent step of the analysis. It may be noted that some of the component edges, especially in the case of hollow sections, cannot shrink freely due to the presence of internal dies. The control volumes along such edges are identified beforehand and are assigned zero-shrinkage properties so that their nodal coordinates remain the same throughout the whole analysis.

3.5 Changes in the material properties

Ignoring the effects of thermal expansion and shrinkage of resin in the longitudinal direction and applying a rule of mixture based on volume fractions (v), the density of material content of control volume j is calculated as:

$$\rho_c^j = v_r \left[\frac{\rho_r}{\left(\delta_r^j\right)^2} \right] + v_f \rho_f \tag{14}$$

where, subscript f refers to fibre reinforcement.

Thermal properties of a composites contained in control volume j are calculated after every time step using rules of mixture based on final DOC and mass fractions (m) as:

$$C_{pc}^{j} = m_r\left[(1-\alpha_T^j)C_{pr}^{u} + \alpha_T^j C_{pr}^{s}\right] + m_f C_{pf} \tag{15}$$

$$\frac{1}{\bar{k}_c^j} = \frac{m_f}{\bar{k}_f} + \frac{m_r}{\left[(1-\alpha_T^j)k_r^u + \alpha_T^j k_r^s\right]} \tag{16}$$

where, $m_f = v_f(\frac{\rho_f}{\rho_c})$, $m_r = 1 - m_f$, and superscripts u and s represent uncured and fully cured resin respectively.

These properties are subsequently converted to FE properties for heat transfer analysis. Depending upon the contribution of various control volumes to a finite element, the properties of the control volumes are volume-averaged to get the properties of the finite element.

3.6 Heat transfer at die-component interface

In the present approach, the heat transfer between the component and the die is modelled using thermal surfaces [13]. These are the thermal equivalent of structural slide-lines and are utilized to model the flow of heat between surfaces that are apart or are in contact.

When the surfaces are in contact (i.e. the corresponding FE nodes have the same coordinates), conduction is considered as the dominant source of heat transfer. When the surfaces are separated from each other by a narrow gap between them, thermal links are set up between the corresponding FE nodes. These thermal link finite elements affect the heat transfer by conduction and/or convection. Heat transfer due to radiation is ignored. The thermal conductivity and the coefficient of convective heat transfer for a thermal link can be defined as a function of the length of the link element. Thus, if the gap is too large, no heat flow is permitted between the surfaces.

While modelling the pultrusion process, thermal surfaces are defined along the peripheral surfaces of the die and the component that are initially in contact with each other. Thus, during the initial stages heat energy is transferred to the component by conduction.

When the component starts to cure, its dimensions change. The new locations of the FE nodes on the periphery of the component describe the size of the gap created at the die-component interface after each time step. Depending upon the size of the gap, the node-to-node heat transfer properties of the thermal surfaces are re-defined. Thus, the present approach can cater for a gap of a different size at different locations. This is necessary when cross-section of a component is irregular and hollow and, uneven dimensional changes and heat transfer across the die-component interface are expected.

4. CASE STUDIES

The developed simulation procedure was used for studying the pultrusion of a rectangular flat, a bridge deck section and a cylindrical rod. The example on a rectangular flat was selected from [2] and was used for validation purposes. The simulation of the bridge deck was designed to illustrate the application of the developed procedure for modelling irregular and hollow sections. The necessary data for the cylindrical rod analysis was taken from [3]. The example was used to further validate the developed procedure and to examine the effects of temperature-dependent properties.

The FE details of the pultrusion die and the rectangular flat are shown in Figure 2. Due to symmetry, only a quarter of the rectangular-flat-die assembly was modelled using 2623 solid field elements. Similar details for the bridge deck section are shown in Figure 3. For the bridge deck, a total of 1488 hexahedron (HX8) and 48 pentahedron (PN6) elements were used to model the part, and, 2880 HX8 and 48 PN6 elements were used to model the die. The boundary of the rectangular flat (Figure 2a) and, the inner and outer surfaces of the bridge deck section shown in Figure 3b, describe the thermal surfaces that affect the heat transfer between the die and the part.

For both components, fiberglass reinforcement was used. In both cases, the heating was affected using six heating pads placed symmetrically on the top and the bottom surfaces of the die; refer Figure 3a for details. In order to achieve the required die temperature, a heating power of *900W* was supplied to each heating-pad. The feedback thermocouple mounted at the centre of each heating pad was used to control temperature at the die surface within a tolerance of $\pm 1\,°C$. During pultrusion, some portion of the die under the leading set of heaters is intentionally cooled to prevent early gelation of the resin [4], which might clog the die entrance. The effect of such cooling was simulated by a heat sink maintained at $50°C$ for the first 100*mm* under the first pair of die-heaters [2]. In case of the rectangular flat, the heat sink was provided along the sections 1-1 and 2-2 shown in Figure 2a. For the bridge deck, however, a square heat sink of $50.8mm \text{ X } 50.8mm$ was assumed. A heat transfer coefficient of $10W/m^2°C$ was used to model the convective heat loss from non-insulated surfaces of the die to the environment $(30°C)$. The heat loss due to radiative heat transfer was ignored. As dictated by the geometry, the bridge deck section required an additional die at the core, see Figure 3. However, no heat source was provided in the core (or internal) die.

The geometrical details of the cylindrical rod are shown in Figure 4. Hercules AS4-12K carbon fibre reinforcement was used for fabricating the cylindrical rod. A steady-state temperature profile based on the experimental work of Valliappan et al. [3] was used to describe the die-wall temperatures. Since thermal loading was constant along the periphery of the rod cross-section, only a segment of the rod defined by an angle of *0.5radians* was modelled.

In all three cases, Crome (5%) steel, *76mm X 76mm X 915mm*, die and SHELL EPON9420/9470/537 epoxy resin system were used. The pull-speed was maintained at *5mm/seconds*. The convergence limits for temperature and DOC were set at *0.005°C* and

0.0005 respectively. The thermo-physical properties of the materials used in all three cases are listed in Table 1. The cure kinetics models, heat of exothermic reaction and % fibre volume content used for the case studies are given in Table 2.

It may be noted that for the bridge deck and the cylindrical rod a linear variation of maximum *25%* was assumed for specific heat and thermal conductivity of the resin between its uncured and fully cured state while studying the effects of temperature dependent properties. The values ε_r and γ_r were taken as $0.000045 mm/mm/^{\circ}C$ and *4.0%* respectively. The thermal surfaces were assumed to be initially in good contact with each other and heat transfer between the composites and the die was considered to be dominated by conduction. As the component separated from the die wall, the gap conductance was reduced linearly it as a function of the size of the gap and that heat flow at the interface was allowed only when the gap was less than *2mm*.

5. RESULTS AND DISCUSSIONS

5.1 Rectangular flat

The comparison between the results of the present analysis with the results reported in [2] is shown in Figure 5. The close agreement between these results indicates that the present simulation procedure is numerically correct and reliable.

5.2 Cylindrical rod

Three FE models with different mesh density (the element size in the pull direction was *4mm*, *8mm* and *16mm* respectively) were used to study the role of Peclet number Pe. The Pe for these three FE models were *42*, *84* and *168* respectively and they had little effect on the final results. The die temperature profile used and the results of the simulation are shown in Figure 6. The results agreed well with the data published in [3].

The same example was further analyzed using temperature-dependent material properties. However the %resin volume content was increased from *37.8%* to *50%* so that the influence of resin properties and their variation with temperature could be examined more effectively.

As seen from Figure 7, the predictions differed significantly from the case when the temperature-dependence of the material properties was not considered during the simulation. It was observed that when the k and C_p of the fully cured resin were *10*% higher than the uncured resin, the peak temperature at the centreline of the rod dropped to *217℃* from *232℃*. However, the temperature profile was similar to that obtained using the constant material properties and the temperature peak was clearly noticeable. The maximum temperature further dropped to *204℃* resulting in a flat temperature profile when a variation of *25*% was assumed between the properties of the uncured and cured resin.

The results show that the increase in the thermal mass due to the increase in the specific heat capacity of the resin with the degree of cure contributed most to the fall in the temperatures of the rod in the zone where the rate of cure reaction was higher. The higher the thermal mass of the resin, the more the heat energy required to raise the temperature of the composites. Similarly, when thermal conductivity of the resin increases with curing, heat energy dissipates more efficiently from high temperature area to low temperature area. This would also depress the temperature peak. Since the die-residence time for the composites and the heat input to the die remained the same, the temperatures of the cylindrical rod reduced with an increase in the thermal properties of the resin. As a consequence, the cure reaction slowed down resulting in DOC profiles with smoother gradients; see Figure 7b. This shows that ignoring the temperature-dependence of the material properties leads to higher estimations of temperatures and degree of cure of the pultrudate.

During simulation the radius of the cylindrical rod at the rear die end was found to have reduced from *4.75mm* to *4.739mm*. This indicates that as it cured the composites section separated from the die wall due to the shrinkage of the resin.

5.3 Bridge deck section

The plots of temperature and DOC measured at points A and B (refer Figure 3b for their locations) as a function of the length of the die are shown in Figure 8. At point A, the results seemed to be significantly affected by the use of temperature-dependent material properties. With a variation of *25*% in the resin properties, the maximum temperature at point A dropped from *192*℃ to *169*℃ and the final DOC by *23*%. Such high variations were seen at point A that lies within the thicker flange of the bridge deck section than at point B located at the top edge of the deck. As discussed earlier in the previous section the specific heat capacity of the resin increased significantly with the degree of cure requiring more and more heat to raise its temperature. Since the heat energy was readily available at point B, the temperature profile was not affected much even though the thermal mass was more. However, since point A was away from the die, the temperatures could not rise as rapidly as at point B. This resulted in a retarded cure reaction and reduced the DOC at point A; see Figure 8b. In addition, as the resin cured its chemical shrinkage led to a maximum of *0.013mm* contraction in the cross-section of the bridge deck in the X direction and *0.008mm* in the Y direction causing the bridge deck to separate from the die at certain locations.

As a consequence of all these, the final state of cure of the bridge deck section was different (see Figure 9 for the contour plots) between analyses conducted using temperature-dependent material properties and temperature-independent properties.

This highlights the importance of having a simulation procedure for pultrusion that can account for the changing material properties and heat transfer characteristics at the die-component interface as a function of temperature.

6. CONCLUSIONS

The presented case studies show that the developed FE /NCV procedure is numerically stable, robust and reliable. The various numerical schemes developed to cater for the effects of convective heat transfer, shrinkage and thermal expansion of the resin and, temperature-dependent material properties were compatible with the FE/NCV concept. The developed procedure can be successfully used for three-dimensional simulation of pultrusion of various composites components, including hollow and irregular sections. However, the numerical predictions could be inaccurate when temperature-dependence of the material properties is ignored during simulation.

REFERENCES

1. Suratno B.R., Ye L., Mai Y.W., Simulation of temperature and curing profiles in pultruded composite rods, *Composites Science and Technology*, Vol. 58, 1998, pp 191-197.
2. X.L. Liu, I.G. Crouch, Y.C. Lam, Simulation of heat transfer and cure in pultrusion using a general-purpose FE package, *Composites Science and Technology*, Vol. 60, No. 6, 1998, pp 857-864.
3. Valliappan M., Roux J.A., Vaughan J.G. and Arafat E.S., Die and post-die temperature and cure in Graphite/Epoxy composites, *Composites: Part B*, Vol. 27B, 1996, pp 1-9.
4. Chachad Y.R., Roux J.A., Vaughan J.G., Thermal model for three-dimensional irregular shaped pultruded fiberglass composites, *Journal of Composites Materials*, Vol. 6, No. 30, 1996, pp 692-721.
5. Hackett R.M., Zhu S.Z., Two-dimensional finite element model of the pultrusion process, *Journal of Reinforced Plastics and Composites*, Vol. 11, December 1992, pp 1322-1351.
6. Joshi S.C., Liu X.L., Lam Y.C., A numerical approach for modelling of polymer curing in fibre reinforced composites, *Composites Science and Technology*, Volume 59, No. 7, 1999, pp 1003-1013.
7. Y.C. Lam, Sunil C. Joshi and X.L. Liu, Numerical simulation of mould-filling process in resin transfer moulding, *Composites Science and Technology*, Vol. 60, No. 6, 1998, pp 845-855.
8. Joshi S.C., Lam Y.C. and Liu X.L., Mass conservation in numerical simulation of resin flow, *Composites A: Applied Science and Manufacturing*, Vol. 31, No. 10, 2000, pp 1061-1068.
9. Joshi S.C., Liu X.L., Lam Y.C. and Sheridan J., Simulation of resin film infusion process using finite element/ nodal control volume approach, *Advanced Composites Letters*, Volume 8, Issue 3, 1999, pp 101-104.
10. Rudd C.D., Long A.C., Kendall K.N., Mangin C.G.E., *Liquid Moulding Technologies*, ed. I, Chapter 7: material characterisation, Woodhead publishing limited, Cambridge, England, 1997, pp 241-247.
11. Batch G.L., Macosko C.W., Heat transfer and cure in pultrusion: model and experimental verification, *American Institute of Chemical Engineers Journal*, Vol. 39, No. 7, July 1993, pp 1228-1241.
12. Fuller A.J. Baden, *Engineering Field Theory*, Pergamon press, 1973, p 11.
13. LUSAS version 13.0, *Theory & User's manuals*, FEA Limited, Surrey, UK.

LIST OF FIGURES

LIST OF TABLES

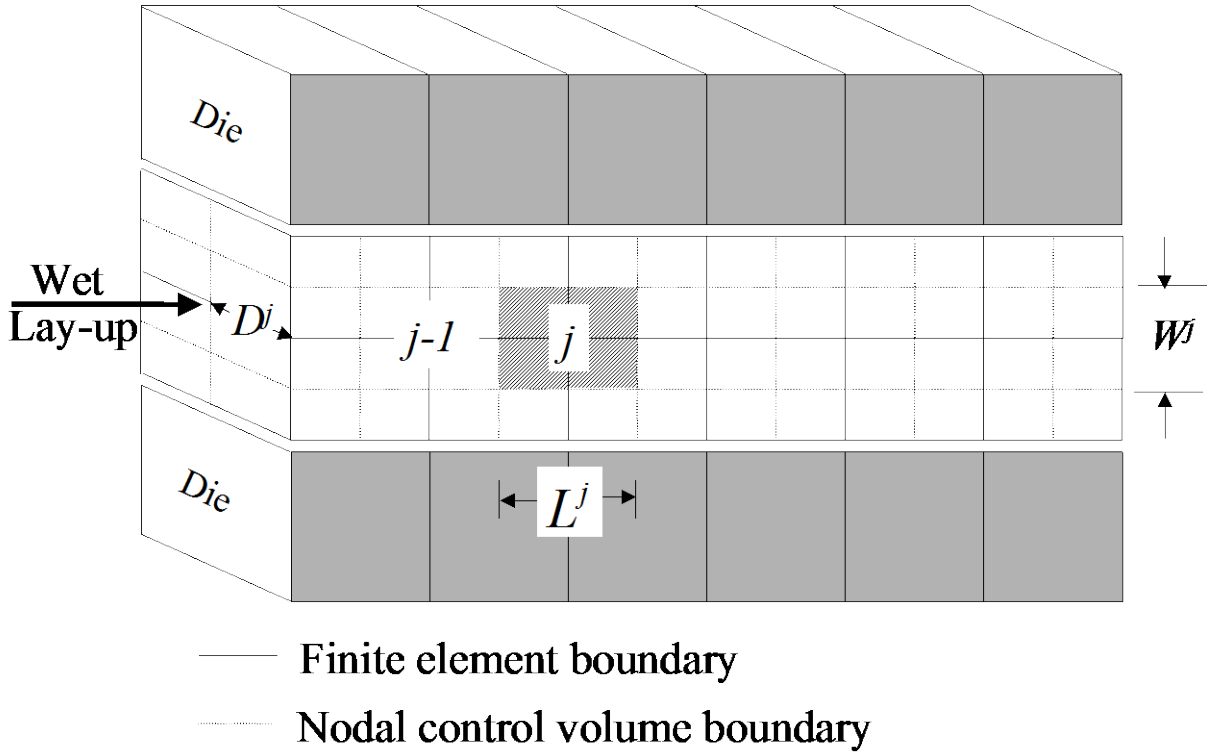

Figure 1 *FE/ NCV model of pultrusion die.*

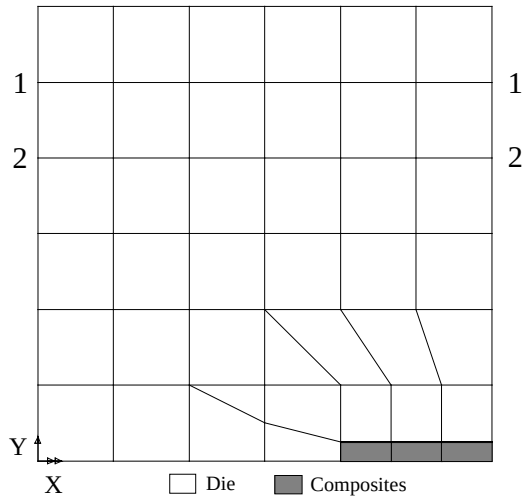

(a) *Cross-sectional details*

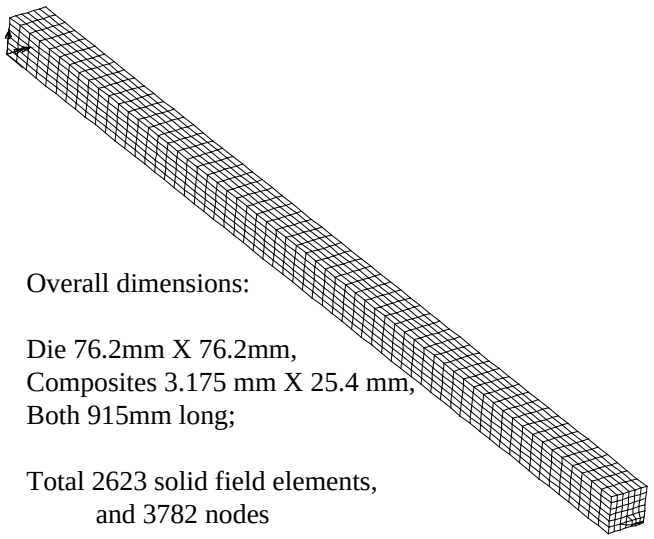

(b) *Complete FE model*

Figure 2 *FE model of pultrusion die for the rectangular flat.*

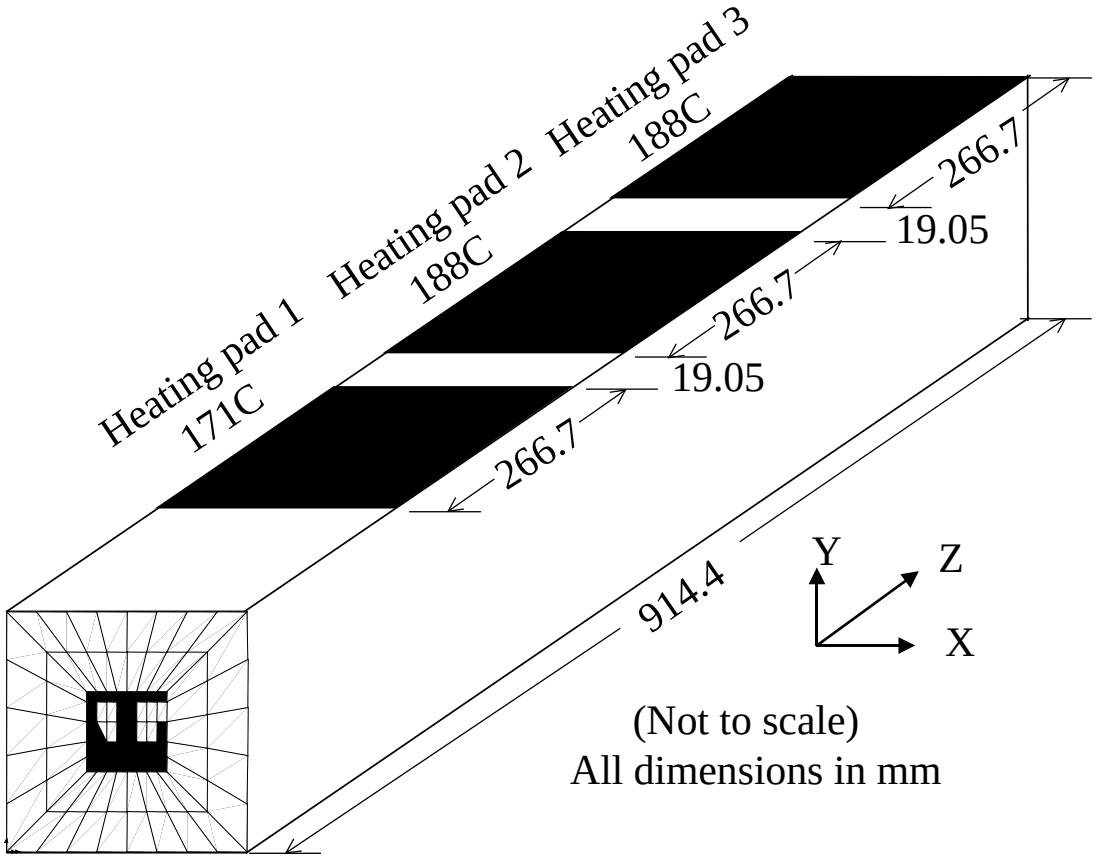

(a) *Geometrical details of the die and the heater arrangement*

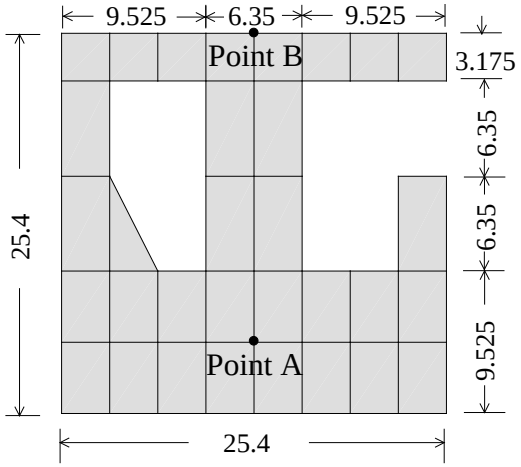

(b) *Cross-section of the bridge deck*

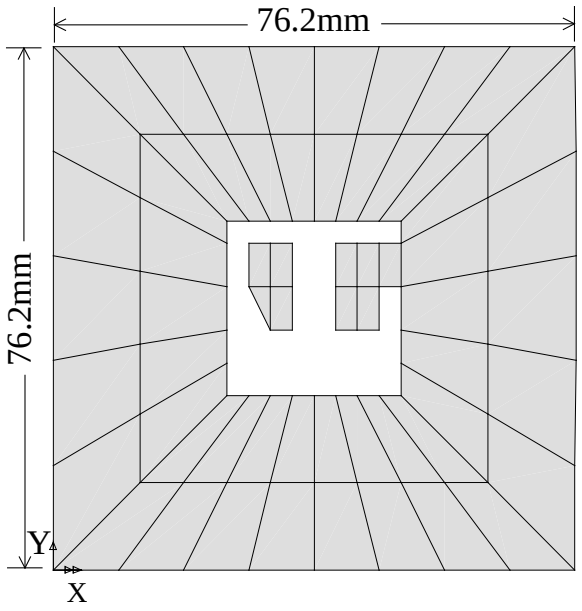

(c) *Cross-section of the die*

Figure 3 *FE models and other details of the pultrusion die and bridge deck.*

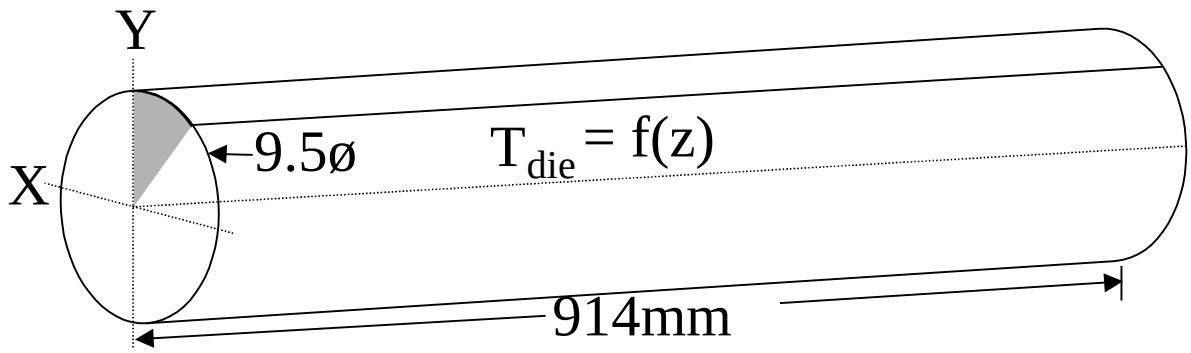

Figure 4 *Details of the cylindrical rod.*

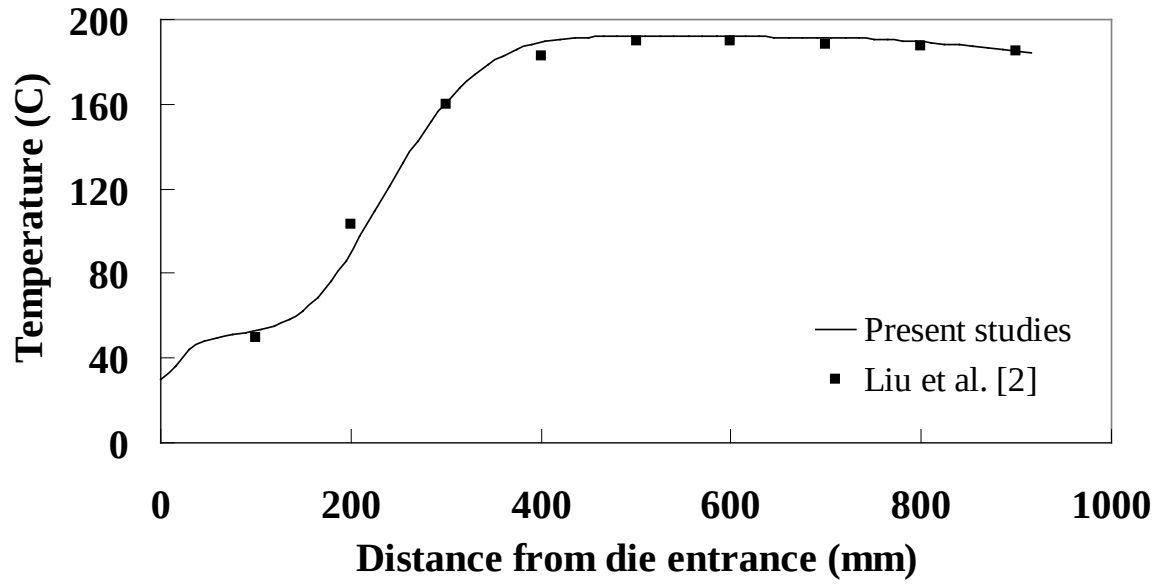

a)

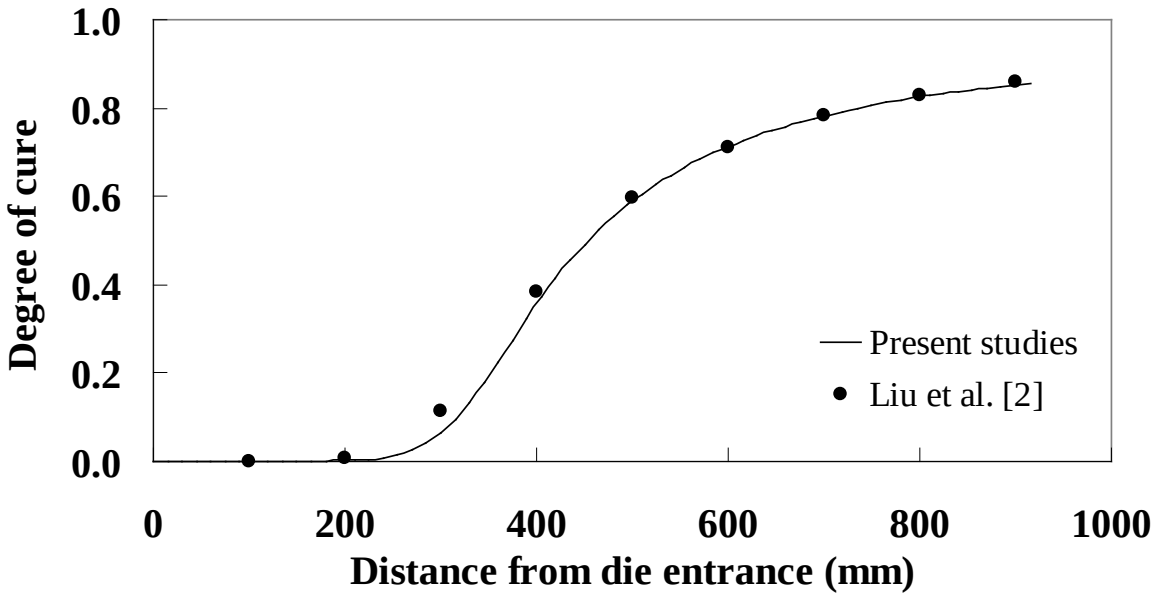

(b)

Figure 5 *Predicted centreline temperature and DOC profiles for the rectangular flat and their comparison with published data.*

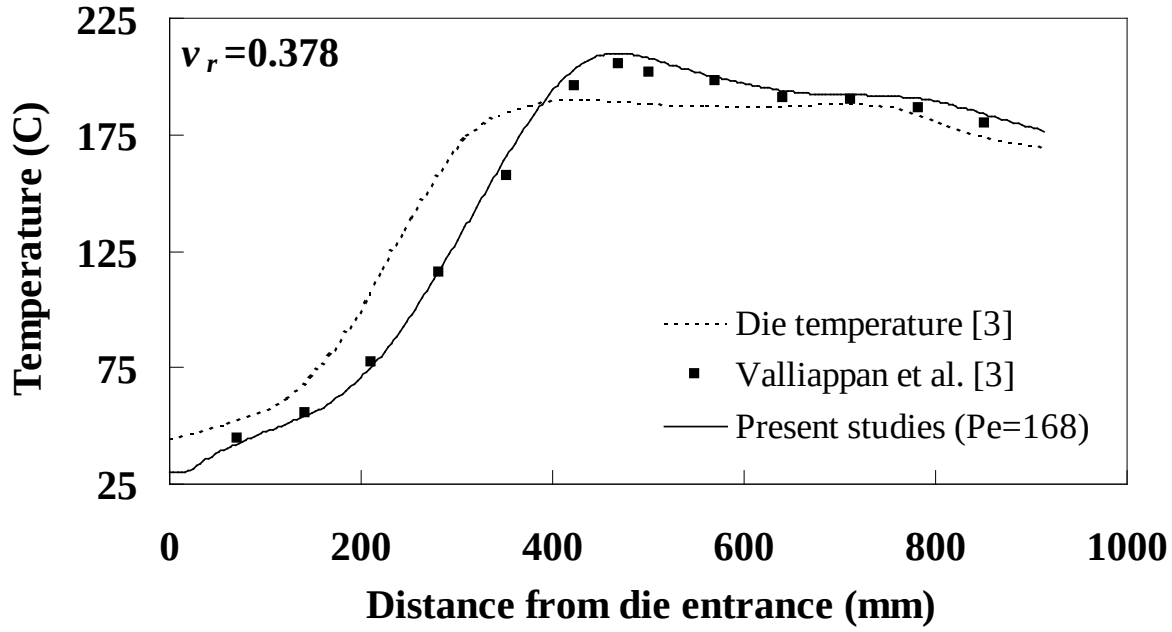

(a)

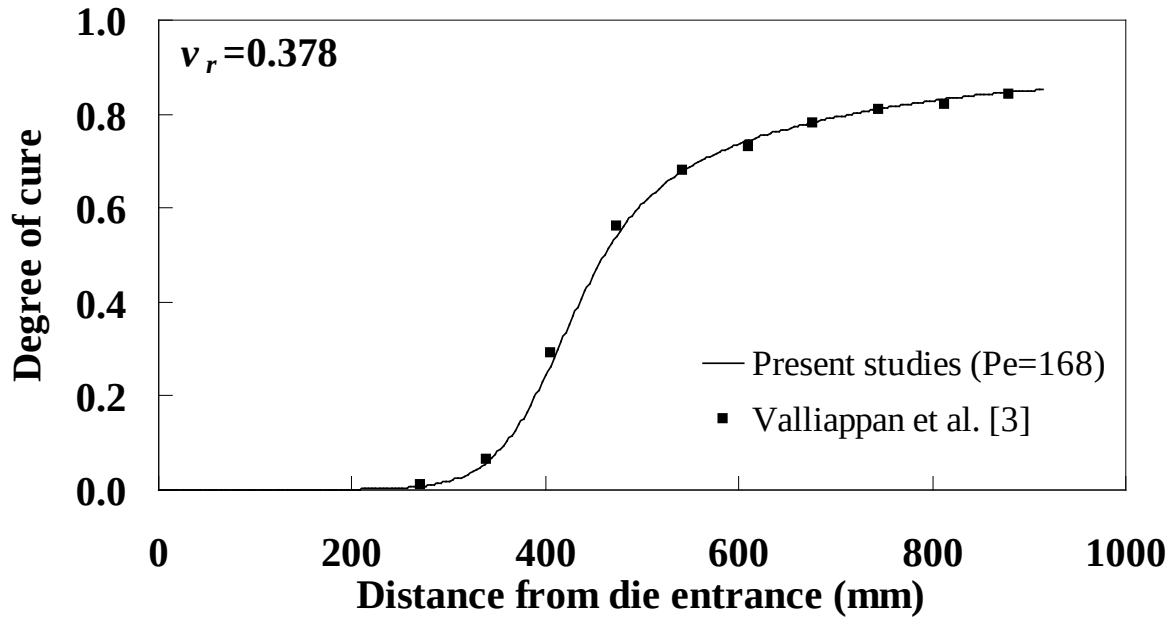

(b)

Figure 6 *Die temperature profile used for the simulation of cylindrical rod, and predicted centreline temperature and DOC profiles with their comparison with published data.*

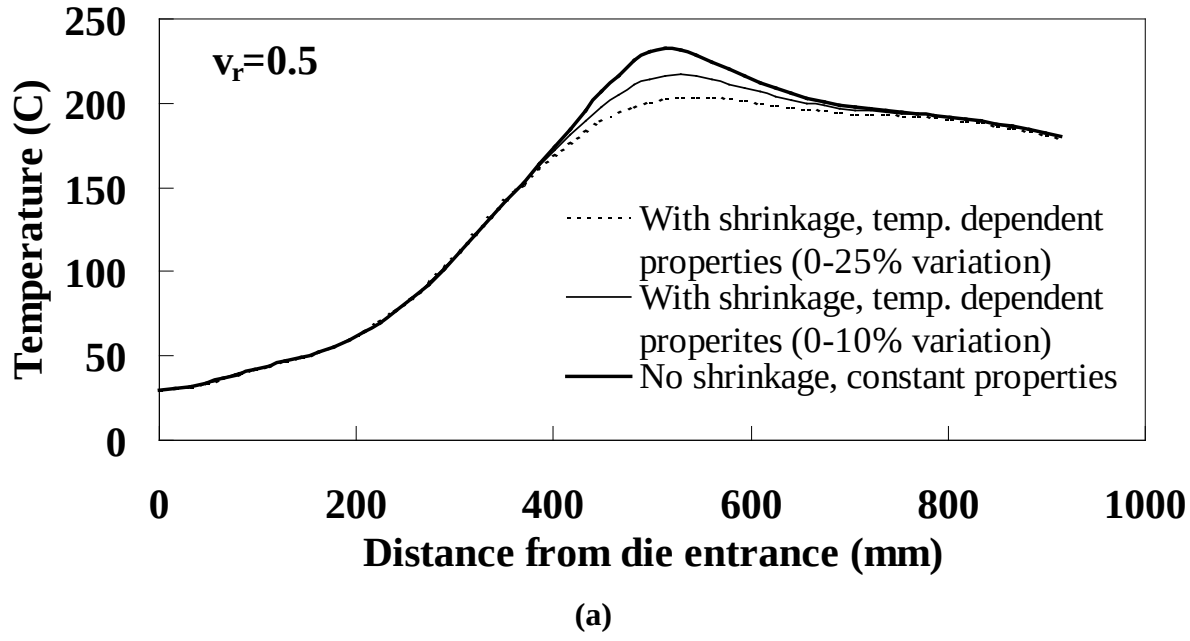

(a)

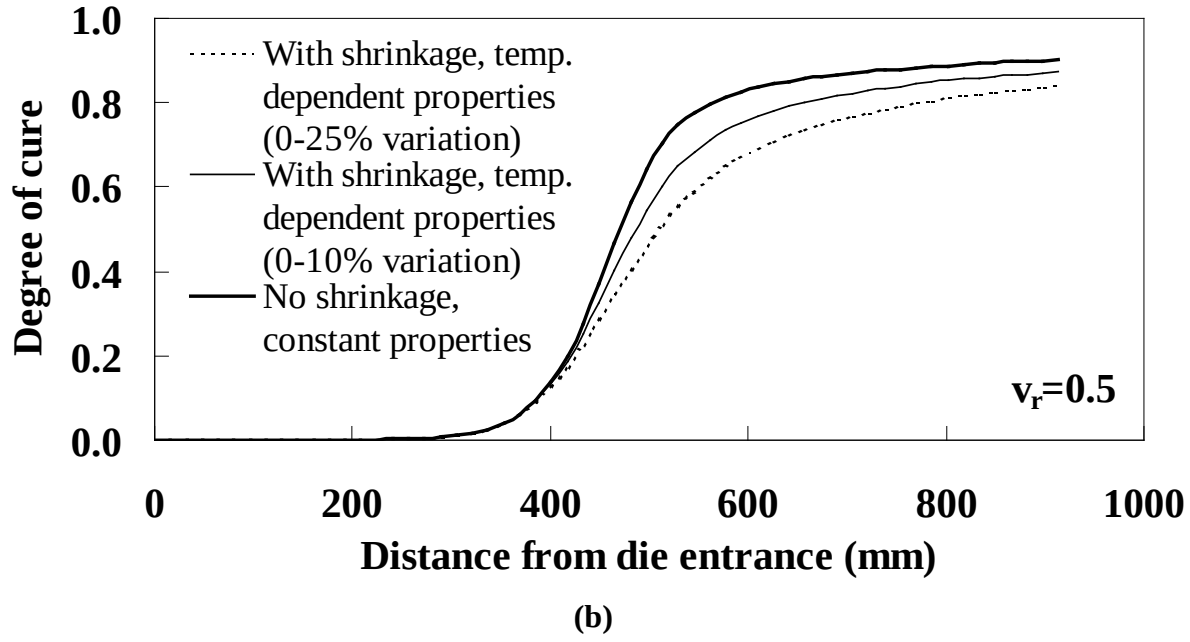

(b)

Figure 7 *Effect of temperature-dependent properties, including chemical shrinkage of resin, on centreline temperature and DOC for the cylindrical rod.*

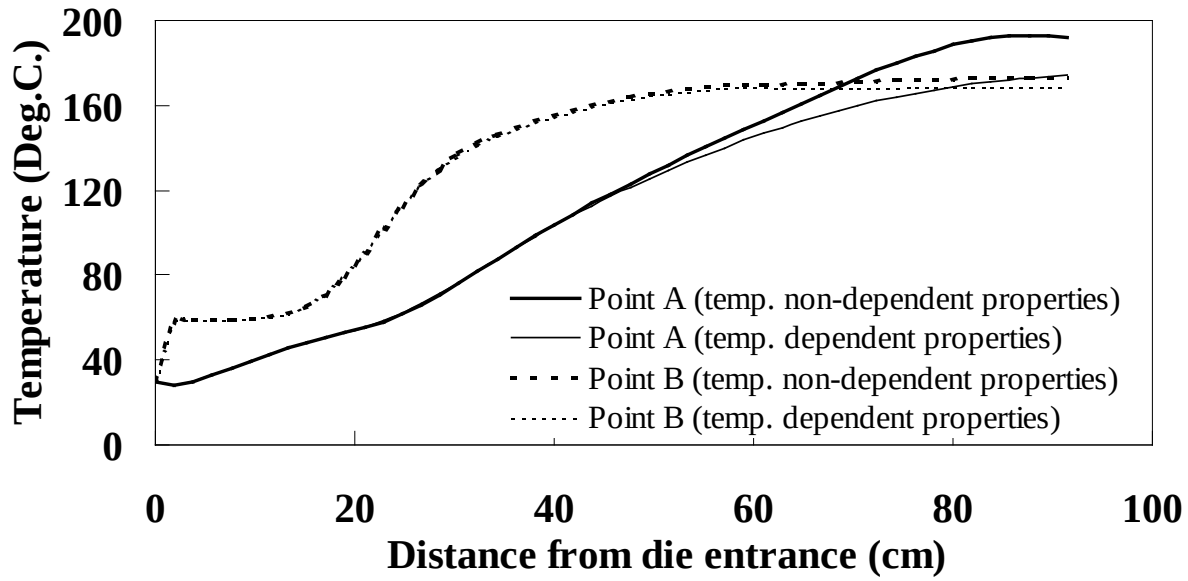

(a)

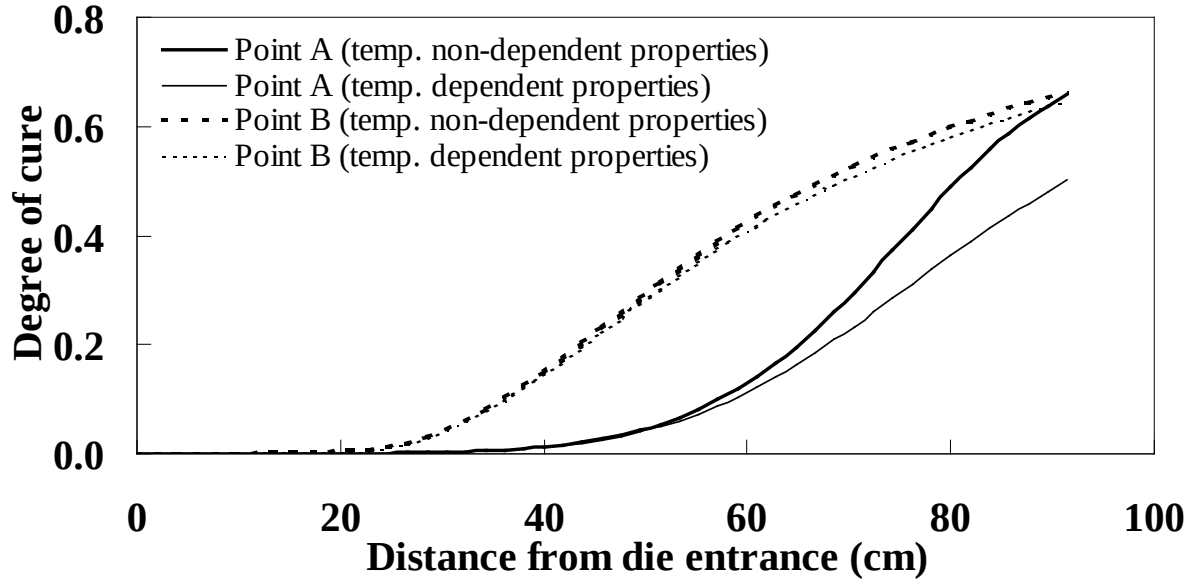

(b)

Figure 8 *Temperature and DOC profiles for the bridge deck section.*

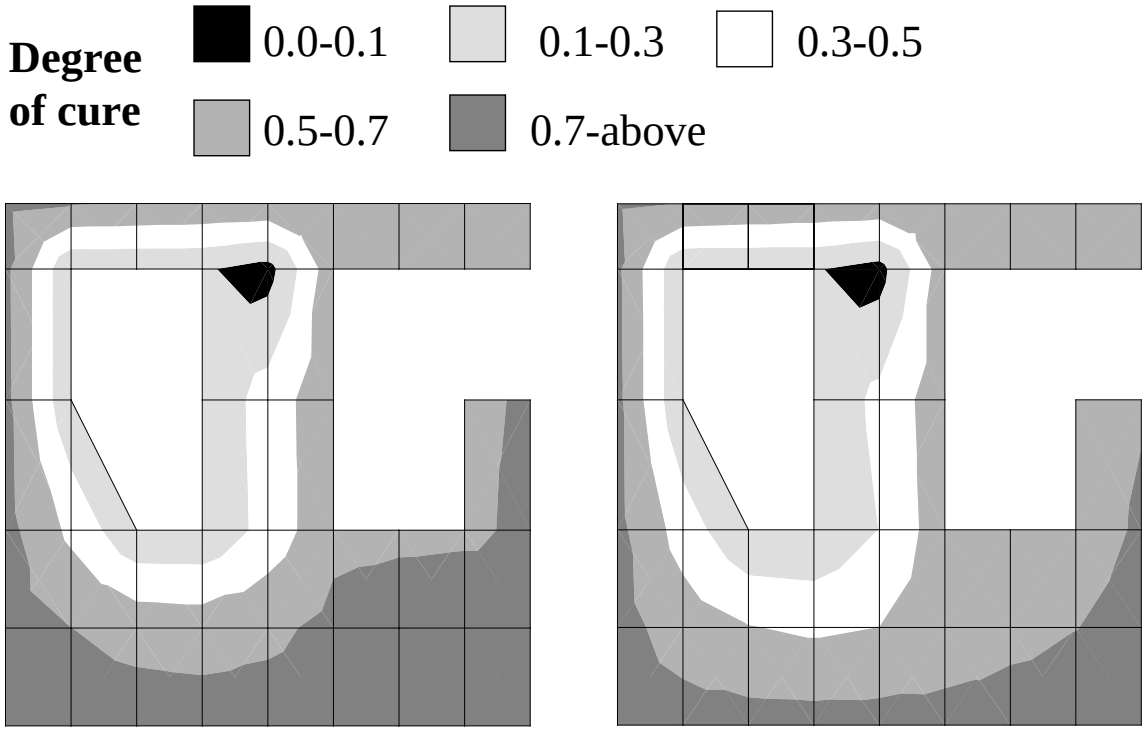

(a) *without temperature-dependent material properties*

(b) *with temperature-dependent material properties*

Figure 9 *The final state of cure of the bridge deck section.*

Table 1. *Material properties used for the analysis.*

Material	**Density** ρ **(*kg/m*^{3})**	**Specific heat** C_p **(*J/kg.K*)**	**Thermal conductivity** k **(*w/m.K*)**
Crome steel	7833	460	40 [4]
Resin [2,3]$^+$	1260$^+$	1255$^+$	0.21 (rectangular flat), 0.20$^+$ (Cylindrical rod and bridge deck)
Fully cured resin (C_p and λ 10% higher than uncured resin)	1312.5 (with 4% chemical shrinkage)	1380.5	0.22
Fully cured resin (C_p and λ 25% higher than uncured resin)	1312.5 (with 4% chemical shrinkage)	1568.75	0.25
Glass fibres [2,4]	2560	670	$k_{longitudinal}$ = 11.4, $k_{crossfibre}$ = 1.04
Carbon fibres [3]	1790	712	$k_{longitudinal}$ = 66, $k_{crossfibre}$ = 11.6

$^+$ These properties were considered as the equivalent temperature-independent properties. However, for some of the analyses as stated in the text, these were treated as the properties of the uncured resin.

Table 2 *Cure kinetics parameters, heat of reaction for* EPON 9420/9470/537 *epoxy resin system and % fibre volume contents used in the present studies.*

Component	**Arrehenius equation**	**Total heat of reaction H_t (*J/gm*)**	**% Fiber volume content**
Rectangular flat [2]	$\frac{d\alpha}{dt} = (1.92\times10^5)e^{(\frac{-6\times10^4}{RT})}(1-\alpha)^{1.69}$	324	63.9
Cylindrical rod [3]	$\frac{d\alpha}{dt} = (1.914\times10^5)e^{(\frac{-6.05\times10^4}{RT})}(1-\alpha)^{1.69}$	323.7	62.2 (for validation) 50.0 (for studies on resin shrinkage)
Bridge deck section	$\frac{d\alpha}{dt} = (1.914\times10^5)e^{(\frac{-6.05\times10^4}{RT})}(1-\alpha)^{1.69}$	323.7	60.0